

Weakly Supervised Gaussian Contrastive Grounding with Large Multimodal Models for Video Question Answering

Haibo Wang, Chenghang Lai, Yixuan Sun, Weifeng Ge[✉]

School of Computer Science, Fudan University

{22210240289, chlai21, 21210860014}@m.fudan.edu.cn, wfge@fudan.edu.cn

Abstract

Video Question Answering (VideoQA) aims to answer natural language questions based on the information observed in videos. Despite the recent success of Large Multimodal Models (LMMs) in image-language understanding and reasoning, they deal with VideoQA insufficiently by simply taking uniformly sampled frames as visual inputs, which ignores question-relevant visual clues. Moreover, there are no human annotations for question-critical timestamps in existing VideoQA datasets. In light of this, we propose a novel weakly supervised framework to enforce the LMMs to reason out the answers with question-critical moments as visual inputs. Specifically, we fuse the question and answer pairs as event descriptions to find multiple keyframes as target moments, which will be pseudo-labels. With these pseudo-labels as additionally weak supervision, we devise a lightweight **G**aussian-based **C**ontrastive **G**rounding (*GCG*) module. *GCG* learns multiple Gaussian functions to characterize the temporal structure of the video, and sample question-critical frames as positive moments to be the visual inputs of LMMs. Extensive experiments on several VideoQA benchmarks verify the effectiveness of our framework, and we achieve substantial improvements compared to previous state-of-the-art methods

1 Introduction

Video Question Answering (VideoQA) stands at the forefront of developing intelligent systems that can reason about causal and temporal relations and answer natural language questions in videos, which is an essential manifestation of human intelligence. Despite significant advancements in recent years, VideoQA remains a challenging problem that requires models to comprehensively understand and dynamically align the semantics of both the visual world and natural language.

[✉] Corresponding Author

Codes will be released after review

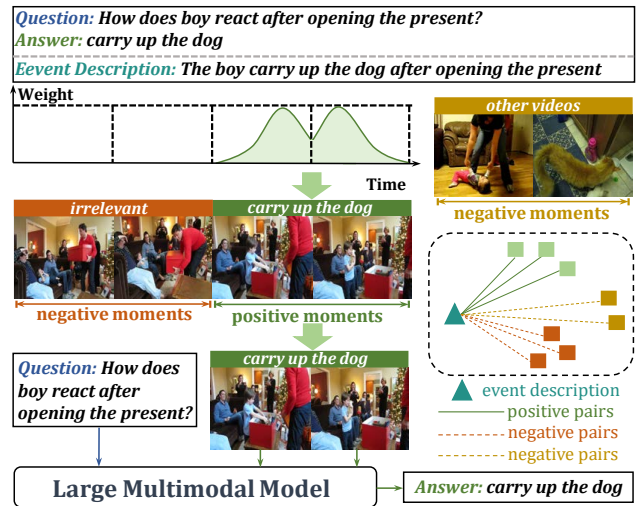


Figure 1: We argue that the information in uniformly sampled frames is insufficient for LMMs to answer the question correctly. Therefore, we utilize the fused event description to provide additional weak supervision and generate weight distributions for each video moment. We align the positive description-moment pairs while pushing away negative ones. In this way, we can effectively select question-critical moments for LMMs to reason out the answer.

With the notable progress in vision-language pre-training techniques [Radford *et al.*, 2021; Li *et al.*, 2022b] and Large Language Models (LLMs) [Touvron *et al.*, 2023; Brown *et al.*, 2020], Large Multimodal Models (LMMs) [Li *et al.*, 2023c; Dai *et al.*, 2023; Liu *et al.*, 2023] have showcased impressive capabilities across various image-language tasks. However, limited by the long sequence frames in videos and computation costs, current LMMs fall short when applied to VideoQA. They simply concatenate the visual tokens of uniformly/randomly sampled, sparse frames (e.g., 4 frames) as the visual inputs for answer prediction. Such a uniform sampling strategy does not consider the specific question, treating all frames equally and introducing redundancy, particularly when tackling complicated questions within longer videos.

Therefore, it's necessary to localize the moments crucial for answering the question for LMMs (as the positive moments shown in Figure 1). Notably, different from the task

of Temporal Sentence Grounding (TSG) [Gao *et al.*, 2017; Zhang *et al.*, 2023] which aims to localize a video moment described by a declarative sentence, the grounding mechanism in VideoQA features some unique challenges. **First**, questions in VideoQA are interrogative sentences, and they lack explicit information about the answer content needed to be grounded. For instance, there is a semantic gap between the interrogative question [How does the boy react after opening the present?] and the declarative description [The boy carries up the dog after opening the present.]. Thus, models are required to both localize the moment [after opening the present] explicitly shown in the question and identify the implicit answer moment [carry up the dog], demanding the causal-temporal reasoning. **Second**, VideoQA aims to correctly answer the questions of videos, rather than solely grounding specific video moments, and there are no human annotations for the timestamps of question-critical moments in existing VideoQA datasets.

To address these challenges, we introduce a weakly supervised framework by discovering question-critical moments with **Gaussian-based Contrastive Grounding (GCG)**. As labeling the timestamps of question-critical moments is labor-intensive and subjective, we leverage the visual-language alignment capability of the CLIP models [Fang *et al.*, 2023] to weakly provide timestamps of question-critical moments. In detail, we fuse the textual question and answer to generate a declarative sentence as the event description, and then compute the similarities between the description and each frame. Frames with the highest scores will be the keyframes of target moments. We observe that LMMs with these keyframes as visual inputs showcased significant improvements in VideoQA datasets. With these pseudo-labeled timestamps as additional weak supervision, our *GCG* will learn multiple Gaussian functions to characterize the inherent temporal structure of the video, and distinguish the positive video moments (green in Figure 1) from negative video moments (orange and yellow in Figure 1). The positive moments are crucial for answering the question and will be the visual inputs of LMMs for final answer prediction. Moreover, to ensure the selected positive moments are closest to the event description, our *GCG* also includes a contrastive objective [He *et al.*, 2020] that can align the positive description-moment pairs while pushing away negative ones. Different from previous works like SeViLA [Yu *et al.*, 2023] which pre-train an additional LMM as the keyframe localizer with other TSG datasets like QV-Highlights [Lei *et al.*, 2021], our method is lightweight for end-to-end training and flexible for LMMs.

To summarize, we make the following contributions:

- We propose a weakly supervised grounding framework for VideoQA, by utilizing the alignment capability of the CLIP models to provide pseudo-labeled timestamps of keyframes without human-labor annotated costs.
- We devise the **Gaussian-based Contrastive Grounding (GCG)** for weakly-grounded selection of question-critical moments, enhancing the efficiency and interpretability of LMMs when applied to VideoQA.
- We conduct extensive experiments to verify the effec-

tiveness of our proposed method, and achieve substantial improvements on six challenging VideoQA benchmarks including NExT-QA, Causal-VidQA, Intent-QA, ActivityNet-QA, MSVD-QA, and MSRVT-QA.

2 Related Works

2.1 Large Multimodal Models (LMMs)

LMMs [Dai *et al.*, 2023; Li *et al.*, 2023c; Ye *et al.*, 2023; Liu *et al.*, 2023; Alayrac *et al.*, 2022] in their current form primarily function as image-to-text generative models, taking images as input and generating text sequences. These models have demonstrated strong capabilities in image-language understanding and reasoning by adapting frozen language models to frozen image encoders with trainable connection modules, following large-scale image-text pretraining. The connection module can either be a transformer-based architecture like Q-former in InstructBLIP and BLIP-2 [Dai *et al.*, 2023; Li *et al.*, 2023c], Perceiver Resampler in Flamingo [Alayrac *et al.*, 2022], or a simple linear layer in LLaVA [Liu *et al.*, 2023]. Most current LMMs are essentially image-based models, and they simply concatenate the visual tokens extracted from uniformly sampled, sparse frames as visual inputs for video-language tasks. This results in a lack of temporal modeling ability and emphasizes the necessity of selecting specific video moments, particularly for addressing the demands of reasoning-based VideoQA tasks. In this paper, our goal is to enhance the causal-temporal reasoning abilities of LMMs without additional pretraining on video-text corpora, by discovering the question-critical moments with our weakly-supervised Gaussian-based Contrastive Grounding.

2.2 Temporal Grounding in VideoQA

Early VideoQA benchmarks [Yu *et al.*, 2019; Xu *et al.*, 2017; Jang *et al.*, 2017] focus on descriptive questions (e.g., [what’s the man doing]) within short video clips, rarely going beyond a recognition of the objects and actions. Instead, more recent VideoQA benchmarks [Li *et al.*, 2022a; Xiao *et al.*, 2021; Li *et al.*, 2023b] like NExT-QA emphasize counterfactual, temporal, and causal reasoning involving multiple entities and relations, demanding the ability to uncover the causes behind specific events within longer videos, necessitating localizing a text query to specific moments.

In light of this, ATP [Buch *et al.*, 2022] utilizes the tool of atemporal probe to select a single frame without temporal information for downstream tasks. MIST [Gao *et al.*, 2023] and TranSTR [Li *et al.*, 2023e] fuse frames with the mechanism of adaptive temporal rationalization and iterative spatial-temporal attention, respectively. NExT-GQA [Xiao *et al.*, 2023] constructs grounding labels in the test set of NExT-QA and uses a single Gaussian mask to fuse frames along the temporal dimension. SeViLA [Yu *et al.*, 2023], similar to us, utilizes the LMM (BLIP-2) for VideoQA. However, SeViLA uses two LMMs to generate pseudo-labels and answer questions respectively, with extra pre-training on TSG datasets [Lei *et al.*, 2021] and a multi-stage training scheme. Different from previous works, we utilize the CLIP [Radford *et al.*, 2021; Fang *et al.*, 2023] models to automatically provide weak supervision for grounding, and our lightweight

GCG module learns multiple Gaussian functions to generate both positive and negative moments in an end-to-end manner, with an additionally contrastive objective to distinguish positive ones from negative ones for frame selection.

3 Preliminary: LMMs for VideoQA

We take InstructBLIP [Dai *et al.*, 2023] as an example to illustrate how LMMs deal with VideoQA. LMMs approach VideoQA as a text generation task conditioned on the question Q and video \mathcal{V} with T frames. Similar to other LMMs, InstructBLIP predicts the answer \mathcal{A} by the following steps:

(1) The Vision Transformer [Dosovitskiy *et al.*, 2021] in EVA-CLIP [Fang *et al.*, 2023] serves as the frozen image encoder to extract embeddings of each frame individually, and obtains $\mathbf{E} = \{\mathbf{e}_1, \mathbf{e}_2, \dots, \mathbf{e}_T\}$, $\mathbf{E} \in \mathbb{R}^{T \times N_I \times D_I}$, $\mathbf{e}_t \in \mathbb{R}^{N_I \times D_I}$, where t denotes the t -th frame, N_I is the patch number of each frame (including the class token), and D_I is the embedding dimension. To mitigate computational costs, existing LMMs uniformly sample K frames ($K \ll T$) to represent the video, resulting in the $\hat{\mathbf{E}} \in \mathbb{R}^{K \times N_I \times D_I}$.

(2) A trainable Q-former serves as the connection module to bridge the modality gap between vision and language. It takes frame embeddings $\hat{\mathbf{E}}$ and outputs a set of fixed-length frame tokens $\mathbf{F} = \{\mathbf{f}_1, \mathbf{f}_2, \dots, \mathbf{f}_K\}$, $\mathbf{F} \in \mathbb{R}^{K \times N_C \times D_C}$, $\mathbf{f}_t \in \mathbb{R}^{N_C \times D_C}$, where N_C is the token number of each frame ($N_C \ll N_I$, e.g., $N_C = 32$ and $N_I = 257$ in InstructBLIP), and D_C is the dimension of the connection module.

(3) Each \mathbf{f}_t in \mathbf{F} are concatenated together to obtain the flattened $\mathbf{F} \in \mathbb{R}^{(K \cdot N_C) \times D_C}$, followed with a fully-connected layer to project \mathbf{F} into the LLM’s dimension D_L . At last, the final projected $\mathbf{F} \in \mathbb{R}^{(K \cdot N_C) \times D_L}$ is fed into the frozen LLM (e.g., FLAN-T5 [Chung *et al.*, 2022] or Vicuna [Zheng *et al.*, 2023]) serving as soft prompts, together with the word embeddings of question Q , to generate the answer text \mathcal{A} .

The model is trained by optimizing the trainable parameters θ of the model P with the autoregressive objective:

$$\mathcal{L}_{vqa} = - \sum_{t=1}^{L_a} \log P_{\theta}(\mathcal{A}_t | \mathcal{A}_{<t}, \mathcal{V}, Q) \quad (1)$$

where \mathcal{A}_t is predicted autoregressively at position t , and L_a is the sequence length of the ground truth answer text \mathcal{A} . Our motivation is to replace the uniformly sampled frames $\hat{\mathbf{E}}$ in step (1) with question-critical frames as visual inputs.

4 Method

Figure 2 (a) gives an overview of our framework. After extracting the embeddings of T frames, our GCG module will select the most question-critical K frames $\hat{\mathbf{E}}$ from \mathbf{E} , as the visual inputs for the LLM. To ensure the selected frames are most relevant to answering the question, the GCG module will be additionally optimized by the pseudo-labels of question-critical moments, resulting in the regression objective \mathcal{L}_{reg} from weakly grounded timestamps, and the contrastive objective \mathcal{L}_{con} aligning the paired description-moment pairs while pushing away unpaired ones.

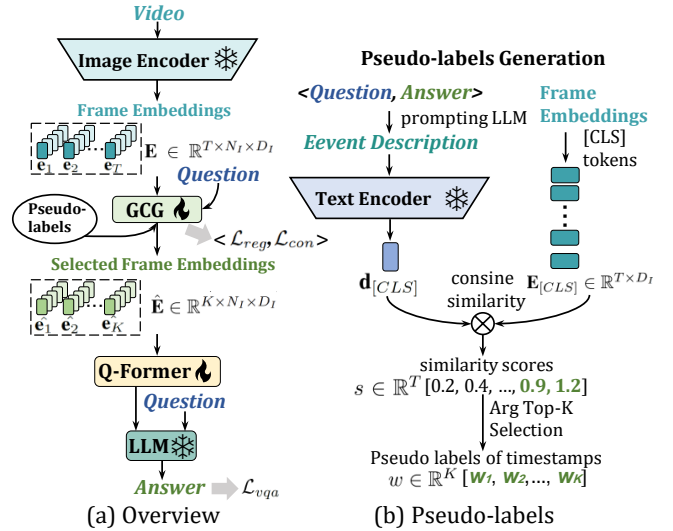


Figure 2: (a) The overall framework of our method. (b) The process of pseudo-label generation.

4.1 Inputs Representation

For video representations, along with the frame embeddings $\mathbf{E} \in \mathbb{R}^{T \times N_I \times D_I}$ extracted in step (1) of Section 3, we also extract the corresponding class tokens $\mathbf{E}_{[CLS]} \in \mathbb{R}^{T \times D_I}$ from \mathbf{E} for further pseudo-labels generation and contrastive grounding. For language representations, we tokenize the question Q into a sequence of words and then feed them into the text encoder of EVA-CLIP, to get word-level embeddings $\mathbf{Q} = \{\mathbf{q}_t\}_{t=1}^{L_q} \in \mathbb{R}^{L_q \times D_I}$, where L_q denotes the sequence length of the question. We get the embeddings of the fused event description (detailed in 4.2) the same way as \mathbf{Q} , but only retain the class token $\mathbf{d}_{[CLS]} \in \mathbb{R}^{D_I}$ to represent it for further pseudo-labels generation.

4.2 Pseudo Labels for Temporal Grounding

Considering the powerful visual-language alignment ability of EVA-CLIP, as in Figure 2 (b), we utilize its joint-trained image and text encoder to provide pseudo labels for timestamps of question-critical moments as weak supervision.

Event Description Generation. To adapt the textual representation for better event description and reduce the semantic gaps, we prompt the LLaMA [Touvron *et al.*, 2023] (or any other open-sourced LLM) to fuse the question and answer pairs with hand-written demonstrations. For example, the QA-pair [Q: How does the boy react after opening the present? A: carry up the dog] will be transformed into the declarative event description [The boy carries up the dog after opening the present.]. The event descriptions provide more accurate textual descriptions for question-critical moments because the answer content is included.

Pseudo Labels Generation. As in Figure 2 (b), we represent the video and event description with the class tokens $\mathbf{E}_{[CLS]} \in \mathbb{R}^{T \times D_I}$ and $\mathbf{d}_{[CLS]} \in \mathbb{R}^{D_I}$ respectively, to obtain the weakly labeled question-critical timestamps. In detail, we compute the cosine similarities between $\mathbf{E}_{[CLS]}$

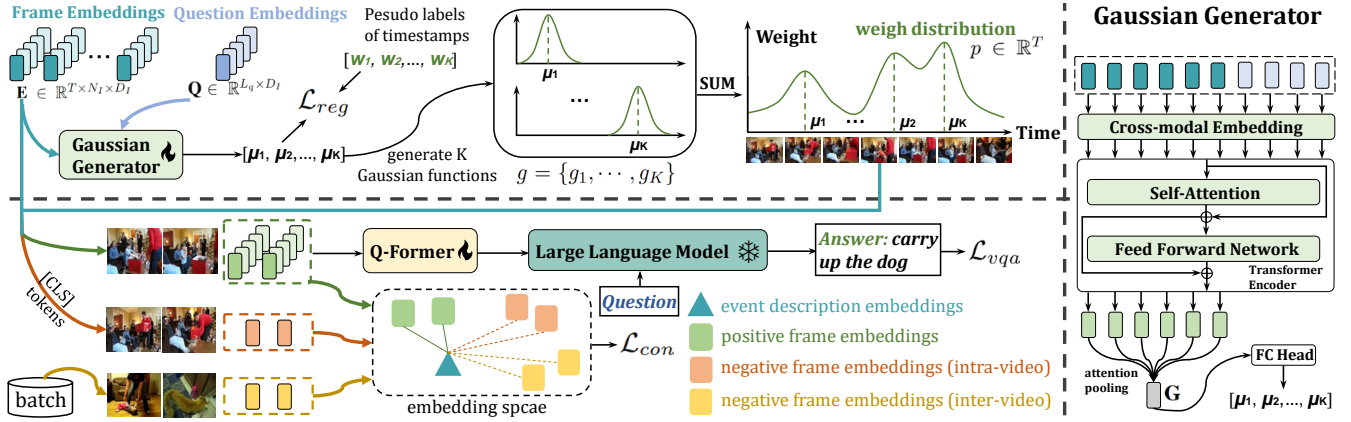


Figure 3: We use the Gaussian generator to generate multiple Gaussian functions and obtain weight distributions $p \in \mathbb{R}^T$ for each video moment. The Gaussian generator will be optimized by the weakly-supervised regression objective \mathcal{L}_{reg} and contrastive objective \mathcal{L}_{con} , along with the fully supervised QA objective \mathcal{L}_{vqa} , to discover the most question-critical moments as visual inputs for LMMs.

and $\mathbf{d}_{[CLS]}$ and get the similarities scores $s \in \mathbb{R}^T$, which recording the relevance between each frame and the event description. Then, we choose the indexes of the highest Top- K scores in s as $w \in \mathbb{R}^K$ where $w_k \in \{1, 2, \dots, T\}$, to be the timestamps of question-critical frames. We verify the effectiveness of the weakly grounded w in the analysis 5.4.

4.3 Gaussian Generator

Recent research [Xiao *et al.*, 2023] highlights the superiority of end-to-end Gaussian mask learning for grounding in VideoQA. Motivated by this, we design the effective weakly supervised Gaussian-based Contrastive Grounding (GCG). However, unlike [Xiao *et al.*, 2023] to generate a single Gaussian function, we generate multiple Gaussian functions to characterize the multi-event temporal structure of the video. Moreover, our GCG is optimized from both the QA supervision \mathcal{L}_{vqa} and weakly labeled supervision, which is more effective for discovering the question-critical moments.

Specifically, we utilize the Gaussian generator to obtain K Gaussian functions $g = \{g_1, \dots, g_K\}$, $g_k \in \mathbb{R}^T$, depending on the video and question. These Gaussian functions will be combined into an overall weight distribution $p \in \mathbb{R}^T$ for each video moment. Notably, p tends to have K peaks, representing the most question-critical K frames, with corresponding indexes to be the centers of each Gaussian function.

As in the right part of Figure 3, the Gaussian generator consists of a cross-modal embedding layer and a transformer encoder [Vaswani *et al.*, 2017]. The cross-modal embedding layer is a down-sampling linear layer with learnable modal-type embeddings and positional embeddings. The concatenated multimodal embeddings $\mathbf{M} = [\mathbf{E}_{[CLS]}; \mathbf{Q}] \in \mathbb{R}^{(T+L_q) \times D_f}$ serve as inputs for the Gaussian generator:

$$\begin{aligned} \mathbf{M} &= \text{Linear}(\mathbf{M}), \mathbf{M} \in \mathbb{R}^{(T+L_q) \times D_G} \\ \mathbf{M}[:, T] &= \mathbf{M}[:, T] + \text{Type}_V + \text{Pos}; \\ \mathbf{M}[T :] &= \mathbf{M}[T :] + \text{Type}_T \end{aligned} \quad (2)$$

Next, a standard transformer encoder is adopted to establish the cross-frame dynamics and cross-modal interactions,

which takes the embedded \mathbf{M} and yields $\hat{\mathbf{M}} \in \mathbb{R}^{T \times D_G}$ (only reserve the first T embeddings). Then, we use attention pooling to summarize the outputs $\hat{\mathbf{M}}$ along the temporal dimension and derive the global video representations $\mathbf{G} \in \mathbb{R}^{D_G}$. As \mathbf{G} integrates all the video and question information, we predict the centers $\mu \in \mathbb{R}^K$ of K learnable Gaussian functions weighting over the entire video sequence, through \mathbf{G} with a fully connected head activated by Sigmoid function:

$$\mu = \text{Sigmoid}(\text{Linear}(\mathbf{G})), \mu \in \mathbb{R}^K \quad (3)$$

Given predicted μ , we get K Gaussian functions $g = \{g_1, \dots, g_K\}$ parameterized with (μ, σ) :

$$\begin{aligned} g_k &= \frac{1}{\sqrt{2\pi}\sigma} \exp\left(-\frac{(t/T - \mu_k)^2}{2\sigma^2}\right), g_k \in \mathbb{R}^T \\ k &= \{1, 2, \dots, K\}, t = \{1, 2, \dots, T\} \end{aligned} \quad (4)$$

where σ is a hyperparameter controlling the width of the Gaussian curve. Then, the weight distribution $p \in \mathbb{R}^T$ of each video moment is generated by summing each g_k :

$$p = \text{Norm}\left(\sum_{k=1}^K g_k\right), p \in \mathbb{R}^T \quad (5)$$

$\text{Norm}(\cdot)$ scales values into the range $[0, 1]$. As the K peaks in p , whose corresponding indexes are $\{\mu_1, \dots, \mu_K\}$, represent the most question-critical K frames, we optimize the Gaussian generator with the regression objective to measure the discrepancy between the predicted centers $\mu \in \mathbb{R}^K$ and the weakly grounded timestamps $w \in \mathbb{R}^K$ by smooth L_1 loss:

$$\mathcal{L}_{reg} = \sum_{k=1}^K \text{Smooth}_{L_1} \|\mu_k - w_k/T\| \quad (6)$$

4.4 Contrastive Grounding

Contrastive grounding aims to ensure the selected moments are most relevant to the event description. To achieve this, we learn a cross-modal embedding space, where the embeddings of the event description $\mathbf{d}_{[CLS]}$ should be well aligned with

the selected positive frames $\mathbf{E}^{pos} \in \mathbb{R}^{K \times D_I}$, which are derived from the weight distribution p , and far away from those irrelevant ones. \mathbf{E}^{pos} are also the class tokens of the selected frame embeddings $\hat{\mathbf{E}} \in \mathbb{R}^{K \times N_I \times D_I}$, which will be the visual inputs of LMMs for final answer prediction.

Positive Moments Selection. Since the distribution p weights each video moment based on its contribution to the question, we select the Top- K elements from $\mathbf{E}_{[CLS]}$ according to p , and obtain $\mathbf{E}^{pos} \in \mathbb{R}^{K \times D_I}$ as the positive frames. However, the selection via vanilla hard Top- K produces a discrete selection, making it inapplicable for end-to-end training. We address this issue by adopting a differentiable Top- K using the perturbed maximum method [Berthet *et al.*, 2020].

Negative Moments Mining. To distinguish highly confusing scenes, we mine negative moments within the same video as intra-negative frames $\mathbf{E}^{intra} \in \mathbb{R}^{N_{intra} \times D_I}$, by sampling frames with the lowest N_{intra} weights in p from $\mathbf{E}_{[CLS]}$. We also use N_{inter} frames randomly sampled from other videos within the same batch to serve as inter-negative frames $\mathbf{E}^{inter} \in \mathbb{R}^{N_{inter} \times D_I}$. These negative samples from both the same video and other videos can provide richer information. The objective of contrastive grounding is described as:

$$\begin{aligned} \mathcal{L}_{con} &= -\frac{1}{K} \sum_{k=1}^K \log \frac{\exp(\mathbf{d}_{[CLS]} \otimes \mathbf{E}_k^{pos} / \tau)}{\exp(\mathbf{d}_{[CLS]} \otimes \mathbf{E}_k^{pos} / \tau) + \text{SUM}} \\ \text{SUM} &= \sum_{i=1}^{N_{intra}} \exp(\mathbf{d}_{[CLS]} \otimes \mathbf{E}_i^{intra} / \tau) + \\ &\quad \sum_{j=1}^{N_{inter}} \exp(\mathbf{d}_{[CLS]} \otimes \mathbf{E}_j^{inter} / \tau) \end{aligned} \quad (7)$$

where τ is the temperature factor and \otimes is the dot product. Contrastive grounding can maximize the similarity between the query $\mathbf{d}_{[CLS]}$ and a group of corresponding positive video moments \mathbf{E}^{pos} under the joint embedding space while pushing away negative video moments.

4.5 Answer Prediction

With the distribution p optimized by both \mathcal{L}_{reg} and \mathcal{L}_{con} , we select the most weighted K frame embeddings from $\mathbf{E} \in \mathbb{R}^{T \times N_I \times D_I}$ based on the p , and obtain the selected frame embeddings $\hat{\mathbf{E}} \in \mathbb{R}^{K \times N_I \times D_I}$. This process replaces the uniform sampling, and the same perturbed maximum method is adopted for differentiability. At last, we feed $\hat{\mathbf{E}}$ into the Q-Former and LLM as the steps (2) and (3) in Section 3 to autoregressively predict the answer \mathcal{A} . During training, the whole pipeline is optimized by the joint objective:

$$\mathcal{L} = \mathcal{L}_{vqa} + \alpha_1 \mathcal{L}_{reg} + \alpha_2 \mathcal{L}_{con} \quad (8)$$

where α_1 and α_2 are the hyper-parameters to control the strengths of GCG . During the inference process, GCG only generates the weight distribution p with the Gaussian generator as in Section 4.3, and obtains the most weighted K frame embeddings $\hat{\mathbf{E}}$ via a fully discrete Top- K selection.

5 Experiments

5.1 Datasets

NExT-QA [Xiao *et al.*, 2021] contains 5.4k videos with an average length of 44s and 52k QA pairs, including question

types of description, causal, and temporal. **Intent-QA** [Li *et al.*, 2023b] focuses on intent reasoning in daily social activities, with more than 4.3k videos and 16k QA pairs, including question types of causal-why, causal-how, and temporal. **Causal-VidQA** [Li *et al.*, 2022a] selects 27k video clips and asks 108k questions, including types of description, explanation, prediction, and counterfactual. **MSVD-QA** and **MSRVTT-QA** [Xu *et al.*, 2017] emphasize the description of video objects, activities, and their attributes, with 50k QA pairs over 1,970 videos and 243K QA pairs over 10K videos respectively. **ActivityNet-QA** [Yu *et al.*, 2019] consists of 58k QA pairs on 5.8k long web videos, with an average length of 180 seconds. NExT-QA, Intent-QA, and Causal-VidQA use a multi-choice setting to test temporal reasoning with causal and commonsense relations. MSVD-QA, MSRVTT-QA, and ActivityNet-QA employ an open-ended setting, focusing on the description of different elements in videos.

5.2 Implementation Details

We choose InstructBLIP [Dai *et al.*, 2023] as our LMM, with EVA-CLIP [Fang *et al.*, 2023] as the image encoder and text encoder, Q-former [Li *et al.*, 2023c] as the connection module, and Vicuna [Zheng *et al.*, 2023] or FLAN-T5 [Chung *et al.*, 2022] as the large language model. We sample each video as a sequence of $T = 32$ frames and select $K = 4$ frames as visual inputs. The number of negative samples is $N_{intra} = 16$ and $N_{inter} = 32$. The number of transformer encoder layers in the Gaussian generator is 2, with the hidden size $D_G = 256$. For the hyperparameters, we set $\sigma = 0.2$, $\tau = 0.1$, $\alpha_1 = \alpha_2 = 0.1$. During training, we keep the parameters of the image encoder, LLM, and text encoder frozen. We use AdamW to optimize the model with a learning rate of $1e^{-5}$ and the strategy of mixed precision.

5.3 Results and Analysis

The experimental results in Table 1 and 2 show the superiority of our weakly-supervised GCG compared to existing approaches. For the multi-choice setting, we achieve an accuracy of 74.6%, 72.1%, and 73.1% in NExT-QA, Causal-VidQA, and Intent-QA respectively. For the open-ended setting, we achieve an accuracy of 61.7%, 49.5%, and 49.9% in MSVD-QA, MSRVTT-QA, and ActivityNet-QA respectively. To ensure a fair comparison, we also apply the same settings to get the results for the vanilla InstructBLIP on these datasets as baselines, with $K = 4$ frames uniformly sampled from the $T = 32$ frames as visual inputs. Although the baseline InstructBLIP performed fair on these datasets, our proposed GCG showed a significant improvement, particularly in questions that require complex causal-temporal reasoning (+2.1% and +2.7% for *Tem* and *Cau* in NExT-QA, +2.3% for *Cou* in Causal-VidQA). Moreover, despite not having undergone video-text pretraining, our method still surpasses those pre-trained VideoQA models (e.g., HiTea, VALOR) on MSVD-QA, MSRVTT-QA, and ActivityNet-QA. We also observe that the improvements on ActivityNet-QA (+3.6%) are larger than the MSVD-QA (+2%) and MSRVTT-QA (+2.5%). This can be attributed to the average video length of ActivityNet-QA being 180 seconds, which is much longer

Method	NExT-QA				Causal-VidQA					Intent-QA			
	<i>Des.</i>	<i>Tem.</i>	<i>Cau.</i>	<i>All</i>	<i>Des.</i>	<i>Exp.</i>	<i>Pre.</i>	<i>Cou.</i>	<i>All</i>	<i>CW.</i>	<i>CH.</i>	<i>Tem.</i>	<i>All</i>
Co-Mem [Gao <i>et al.</i> , 2018]	54.4	50.0	45.9	48.5	64.1	62.8	31.4	32.6	47.7	47.7	54.9	39.1	46.8
HCRN [Le <i>et al.</i> , 2020]	54.0	49.3	47.1	48.9	56.4	61.6	32.6	32.7	48.1	-	-	-	-
HME [Fan <i>et al.</i> , 2019]	57.4	48.9	46.8	49.2	63.4	61.5	28.9	30.9	46.2	46.1	54.3	40.8	46.2
B2A [Park <i>et al.</i> , 2021]	58.3	49.0	47.4	49.6	66.2	62.9	31.2	35.2	49.1	-	-	-	-
HGA [Jiang and Han, 2020]	57.8	49.1	48.1	50.0	65.7	63.5	32.2	34.3	48.9	44.9	51.0	39.6	44.6
IGV [Li <i>et al.</i> , 2022c]	59.6	51.7	48.6	51.3	65.9	62.1	35.0	31.2	48.6	-	-	-	-
HQGA [Xiao <i>et al.</i> , 2022a]	59.4	52.3	49.0	51.8	-	-	-	-	-	48.2	54.3	41.7	47.7
MCR [Zang <i>et al.</i> , 2023]	62.3	52.0	49.2	52.4	67.5	65.6	37.8	33.4	51.1	-	-	-	-
VGTV [Xiao <i>et al.</i> , 2022b]	67.3	54.5	52.8	55.7	70.8	70.3	38.4	42.0	55.4	51.4	56.0	47.6	51.3
CaVIR [Li <i>et al.</i> , 2023b]	-	-	-	-	-	-	-	-	-	58.4	65.5	50.5	57.6
TranSTR [Li <i>et al.</i> , 2023e]	70.0	60.2	59.7	61.5	73.6	75.8	48.9	50.3	62.2	-	-	-	-
SeViLA [Yu <i>et al.</i> , 2023]	-	-	-	71.5	-	-	-	-	-	-	-	-	-
InstructBLIP [Dai <i>et al.</i> , 2023]	79.8	70.5	71.5	72.5	79.5	81.4	64.7	56.8	70.6	73.0	70.2	68.8	71.5
GCG (Ours)	80.7	72.6	74.2	74.6	80.7	82.3	66.5	59.1	72.1	75.0	71.9	69.2	73.1

Table 1: Accuracy (%) on NExT-QA, Causal-VidQA, and Intent-QA. *Des.*, *Tem.*, and *Cau* denote question types of Descriptive, Temporal, and Causal in NExT-QA. *Des.*, *Exp.*, *Pre.*, and *Cou* denote question types of Description, Explanation, Prediction, and Counterfactual in Causal-VidQA. *CW.*, *CH.*, and *Tem* denote question types of Causal Why, Causal How, and Temporal in Intent-QA.

Method	MSVD	MSRVTT	ActivityNet
MHN [Peng <i>et al.</i> , 2022]	40.4	38.6	-
VQA-T [Yang <i>et al.</i> , 2021]	46.3	41.5	38.9
TG-VQA [Li <i>et al.</i> , 2023a]	52.5	46.3	48.3
MuLTI-L [Xu <i>et al.</i> , 2023b]	54.7	47.8	-
FrozenBiLM [Yang <i>et al.</i> , 2022]	54.8	47.0	43.2
UMT-L [Li <i>et al.</i> , 2023d]	55.2	47.1	47.9
InternVideo [Wang <i>et al.</i> , 2022]	55.5	47.1	-
HiTea [Ye <i>et al.</i> , 2022]	55.6	45.9	46.4
mPLUG2 [Xu <i>et al.</i> , 2023a]	58.1	48.0	-
COSA-L [Chen <i>et al.</i> , 2023b]	58.6	48.8	49.2
VALOR-L [Chen <i>et al.</i> , 2023a]	60.0	49.2	48.6
InstructBLIP [Dai <i>et al.</i> , 2023]	59.7	47.0	46.3
GCG (Ours)	61.7	49.5	49.9

Table 2: Accuracy (%) on open-ended VideoQA datasets.

Settings	NExT-QA	Intent-QA	MSVD-QA	MSRVTT-QA
Baseline	72.5	71.5	59.7	47.0
Pseudo-labeled (Q)	72.3(-0.2)	70.3(-1.2)	59.9(+0.2)	47.5(+0.5)
Pseudo-labeled (E)	79.1(+6.6)	78.3(+6.8)	64.3(+4.6)	51.8(+4.8)

Table 3: As a preliminary step, we analyze the performance upper bound with weakly labeled keyframes as visual inputs.

than MSVD-QA (10s) and MSRVTT-QA (15s), demonstrating the necessity of discovering question-critical moments.

5.4 Pseudo-labels Analysis.

We further explore the performance with different frames as visual inputs to verify the pseudo-labeled w : Pseudo-labeled (E) means we choose the K frames whose indexes correspond to $w \in \mathbb{R}^K$ as visual inputs (detailed in Section 4.2). Pseudo-labeled (Q) is obtained the same way as Pseudo-labeled (E) but with the pure question for similarity computation. Baseline means we uniformly sample K frames as visual inputs.

Table 3 shows that Pseudo-labeled (E) exhibits significantly improved performance, particularly in benchmarks featuring longer videos and more complicated questions like NExT-QA and Intent-QA. This verifies the effectiveness of

Settings	NExT-QA				MSVD-QA
	<i>Des.</i>	<i>Tem.</i>	<i>Cau.</i>	<i>All</i>	
Baseline	79.8	70.5	71.5	72.5	59.7
\mathcal{L}_{vqa}	80.3	69.9	72.3	72.9	59.5
$\mathcal{L}_{vqa} + \mathcal{L}_{reg}$	79.3	70.5	73.5	73.6	60.4
$\mathcal{L}_{vqa} + \mathcal{L}_{con}$	80.9	71.4	73.3	74.0	60.7
$\mathcal{L}_{vqa} + \mathcal{L}_{reg} + \mathcal{L}_{con}$	80.7	72.6	74.2	74.6	61.7

Table 4: Ablation studies on loss components of GCG.

using the event description to provide pseudo-labels as weak supervision. Moreover, Pseudo-labeled (E) performs much better than Pseudo-labeled (Q). This can be explained from two perspectives: (1) The event descriptions include the contents of the answers needed to be grounded, filling the semantic gap between the pure question and the answer. (2) The CLIP models are mostly pre-trained on images and declarative texts, therefore the declarative event descriptions are more suitable for similarity computation to decide keyframes.

5.5 Ablation Studies

We investigate the role of our weakly-supervised framework with different variants and hyperparameters of GCG.

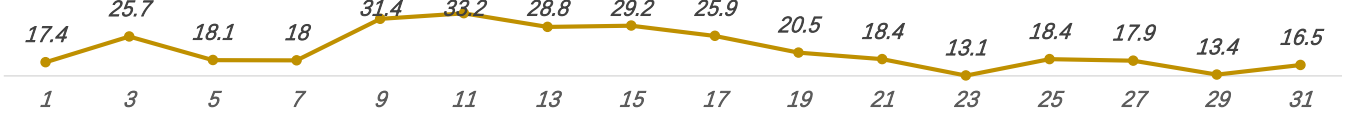
Loss components in GCG. We exhaust the combination of different loss components in GCG. Table 4 shows the results:

- \mathcal{L}_{vqa} solely hardly outperforms the baseline, because the Gaussian generator can not identify the causal scene without supervision of question-critical moments. This reflects our motivation in using the event descriptions to generate pseudo labels as weak supervision.
- $\mathcal{L}_{vqa} + \mathcal{L}_{reg}$ and $\mathcal{L}_{vqa} + \mathcal{L}_{con}$ match equally in accuracy that consistently surpasses baseline and \mathcal{L}_{vqa} . \mathcal{L}_{reg} is responsible for regularizing the indexes of peaks in p to approximate the timestamps of weakly grounded w , and \mathcal{L}_{con} ensures the maximization between the selected moments and event descriptions.
- $\mathcal{L}_{vqa} + \mathcal{L}_{reg} + \mathcal{L}_{con}$ is the complete GCG, which further

Event Description: The baby rolled the roller on the toy when she reached it.



Weakly grounded similarity scores:



Question: what did the baby do when she reached the blue toy?

(A) laugh loudly (B) talk to the other two people (C) rubs face (D) takes a tissue (E) roll the roller on the toy

Prediction with GCG: (E) roll the roller on the toy

Prediction w/o GCG: (A) laugh loudly

Event Description: The baby bit the apple after getting it from the man.



Weakly grounded similarity scores:



Question: what does the baby do after getting the apple from the man?

(A) hit the cake (B) put it to his ear (C) no (D) bite (E) happy

Prediction with GCG: (D) bite

Prediction w/o GCG: (E) happy

Figure 4: Qualitative results on NExT-QA test set. The frames selected by our method are highlighted in blue dashed lines. The ground truth answers are in green. We also display the weakly grounded similarity scores of each frame.

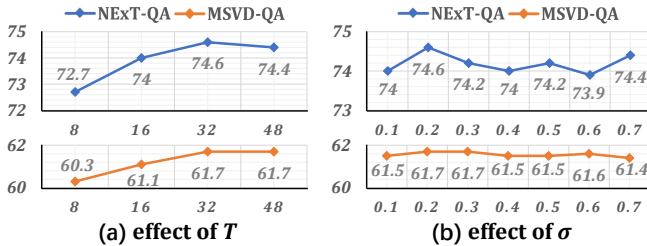


Figure 5: Ablation studies on hyperparameters T and σ .

boosts the performance significantly in all cases, showing that \mathcal{L}_{reg} and \mathcal{L}_{con} contribute in different aspects and their benefits are mutually reinforcing.

Number of frames T and Gaussian widths σ . We evaluate how the number of overall sampled frames T and the widths σ of Gaussian functions will influence the performance. Figure 5 (a) indicates that performance improves as more frames are included, however, beyond a certain threshold ($T = 48$), there is a performance drop. This suggests that too many frames may introduce redundancy and noise, while too few frames miss important information. As for σ in Equation 4, it essentially decides the width and the degree of dispersion of the Gaussian distribution g . A larger σ generates more dispersed g with a more exploratory p and vice versa. In Figure 5 (b), we vary σ from 0.1 to 0.7 and observe that the performance fluctuates in a range of [73.9, 74.6] for NExT-QA and [61.4, 61.7] for MSVD-QA. The performance of NExT-QA is more sensitive to σ , and we argue that this is because the average video length of NExT-QA (44s) is much longer than MSVD-QA (10s).

5.6 Qualitative results.

We also present qualitative results in Figure 4 to gain a clearer insight into our method, along with the frames identified by GCG (bounded with blue dashed lines) and the weakly grounded similarities computed by the event description. Both cases show semantic correspondence between the question and the selected moments. For instance, in the upper case, the frames identified by GCG precisely correspond to the event [The baby rolled the roller on the toy when she reached it] with relatively higher similarity scores, demonstrating the strong ability of our GCG to localize video moments crucial for answering the question. By leveraging the information from this localized segment, the LMM can successfully arrive at the correct answer [roll the roller on the toy]. In contrast, without our GCG , the presence of massive redundancy in the video overwhelms the reasoning process and leads to a false prediction of [laugh loudly].

6 Conclusion

In this paper, we have studied the problem of discovering question-critical moments in videos when adapting LMMs for VideoQA tasks. To address the shortcomings of the uniform sampling strategy and the absence of human annotations for question-critical timestamps in VideoQA datasets, we introduce a weakly-supervised framework to force the LMMs to reason out the answers by grounding question-critical moments. We propose the Gaussian-based Contrastive Grounding, a flexible and lightweight method to dynamically select keyframes with end-to-end training. Through a series of experiments and analyses, we have demonstrated the effectiveness of our approach in various challenging VideoQA tasks,

particularly excelling in causal-temporal reasoning. For future work, we intend to focus on mitigating the biases and superficial correlations observed in previous studies, and further enhance the reasoning abilities of current models.

References

- [Alayrac *et al.*, 2022] Jean-Baptiste Alayrac, Jeff Donahue, Pauline Luc, Antoine Miech, Iain Barr, Yana Hasson, Karel Lenc, Arthur Mensch, Katherine Millican, Malcolm Reynolds, et al. Flamingo: a visual language model for few-shot learning. In *NeurIPS*, 2022.
- [Berthet *et al.*, 2020] Quentin Berthet, Mathieu Blondel, Olivier Teboul, Marco Cuturi, Jean-Philippe Vert, and Francis Bach. Learning with differentiable perturbed optimizers. In *NeurIPS*, 2020.
- [Brown *et al.*, 2020] Tom Brown, Benjamin Mann, Nick Ryder, Melanie Subbiah, Jared D Kaplan, Prafulla Dhariwal, Arvind Neelakantan, Pranav Shyam, Girish Sastry, Amanda Askell, et al. Language models are few-shot learners. In *NeurIPS*, 2020.
- [Buch *et al.*, 2022] Shyamal Buch, Cristóbal Eyzaguirre, Adrien Gaidon, Jiajun Wu, Li Fei-Fei, and Juan Carlos Niebles. Revisiting the” video” in video-language understanding. In *CVPR*, 2022.
- [Chen *et al.*, 2023a] Sihan Chen, Xingjian He, Longteng Guo, Xinxin Zhu, Weining Wang, Jinhui Tang, and Jing Liu. Valor: Vision-audio-language omni-perception pretraining model and dataset. *arXiv preprint arXiv:2304.08345*, 2023.
- [Chen *et al.*, 2023b] Sihan Chen, Xingjian He, Handong Li, Xiaojie Jin, Jiashi Feng, and Jing Liu. Cosa: Concatenated sample pretrained vision-language foundation model. *arXiv preprint arXiv:2306.09085*, 2023.
- [Chung *et al.*, 2022] Hyung Won Chung, Le Hou, Shayne Longpre, Barret Zoph, Yi Tay, William Fedus, Yunxuan Li, Xuezhi Wang, Mostafa Dehghani, Siddhartha Brahma, Albert Webson, Shixiang Shane Gu, Zhuyun Dai, Mirac Suzgun, Xinyun Chen, Aakanksha Chowdhery, Alex Castro-Ros, Marie Pellat, Kevin Robinson, Dasha Valter, Sharan Narang, Gaurav Mishra, Adams Yu, Vincent Zhao, Yanping Huang, Andrew Dai, Hongkun Yu, Slav Petrov, Ed H. Chi, Jeff Dean, Jacob Devlin, Adam Roberts, Denny Zhou, Quoc V. Le, and Jason Wei. Scaling instruction-finetuned language models. *arXiv preprint arXiv:2210.11416*, 2022.
- [Dai *et al.*, 2023] Wenliang Dai, Junnan Li, Dongxu Li, Anthony Meng Huat Tiong, Junqi Zhao, Weisheng Wang, Boyang Li, Pascale Fung, and Steven Hoi. Instructblip: Towards general-purpose vision-language models with instruction tuning. In *NeurIPS*, 2023.
- [Dosovitskiy *et al.*, 2021] Alexey Dosovitskiy, Lucas Beyer, Alexander Kolesnikov, Dirk Weissenborn, Xiaohua Zhai, Thomas Unterthiner, Mostafa Dehghani, Matthias Minderer, Georg Heigold, Sylvain Gelly, et al. An image is worth 16x16 words: Transformers for image recognition at scale. In *ICLR*, 2021.
- [Fan *et al.*, 2019] Chenyou Fan, Xiaofan Zhang, Shu Zhang, Wensheng Wang, Chi Zhang, and Heng Huang. Heterogeneous memory enhanced multimodal attention model for video question answering. In *CVPR*, pages 1999–2007, 2019.
- [Fang *et al.*, 2023] Yuxin Fang, Wen Wang, Binhui Xie, Quan Sun, Ledell Wu, Xinggang Wang, Tiejun Huang, Xinlong Wang, and Yue Cao. Eva: Exploring the limits of masked visual representation learning at scale. In *CVPR*, 2023.
- [Gao *et al.*, 2017] Jiyang Gao, Chen Sun, Zhenheng Yang, and Ram Nevatia. Tall: Temporal activity localization via language query. In *ICCV*, 2017.
- [Gao *et al.*, 2018] Jiyang Gao, Runzhou Ge, Kan Chen, and Ram Nevatia. Motion-appearance co-memory networks for video question answering. In *CVPR*, 2018.
- [Gao *et al.*, 2023] Difei Gao, Luowei Zhou, Lei Ji, Linchao Zhu, Yi Yang, and Mike Zheng Shou. Mist: Multi-modal iterative spatial-temporal transformer for long-form video question answering. In *CVPR*, 2023.
- [He *et al.*, 2020] Kaiming He, Haoqi Fan, Yuxin Wu, Saining Xie, and Ross Girshick. Momentum contrast for unsupervised visual representation learning. In *CVPR*, 2020.
- [Jang *et al.*, 2017] Yunseok Jang, Yale Song, Youngjae Yu, Youngjin Kim, and Gunhee Kim. Tgif-qa: Toward spatio-temporal reasoning in visual question answering. In *CVPR*, 2017.
- [Jiang and Han, 2020] Pin Jiang and Yahong Han. Reasoning with heterogeneous graph alignment for video question answering. In *AAAI*, 2020.
- [Le *et al.*, 2020] Thao Minh Le, Vuong Le, Svetha Venkatesh, and Truyen Tran. Hierarchical conditional relation networks for video question answering. In *CVPR*, 2020.
- [Lei *et al.*, 2021] Jie Lei, Tamara L Berg, and Mohit Bansal. Detecting moments and highlights in videos via natural language queries. In *NeurIPS*, 2021.
- [Li *et al.*, 2022a] Jiangtong Li, Li Niu, and Liqing Zhang. From representation to reasoning: Towards both evidence and commonsense reasoning for video question-answering. In *CVPR*, 2022.
- [Li *et al.*, 2022b] Junnan Li, Dongxu Li, Caiming Xiong, and Steven Hoi. Blip: Bootstrapping language-image pre-training for unified vision-language understanding and generation. In *ICML*, 2022.
- [Li *et al.*, 2022c] Yicong Li, Xiang Wang, Junbin Xiao, Wei Ji, and Tat-Seng Chua. Invariant grounding for video question answering. In *CVPR*, 2022.
- [Li *et al.*, 2023a] Hao Li, Peng Jin, Zesen Cheng, Songyang Zhang, Kai Chen, Zhennan Wang, Chang Liu, and Jie Chen. Tg-vqa: Ternary game of video question answering. In *IJCAI*, 2023.
- [Li *et al.*, 2023b] Jiapeng Li, Ping Wei, Wenjuan Han, and Lifeng Fan. Intentqa: Context-aware video intent reasoning. In *ICCV*, 2023.

- [Li *et al.*, 2023c] Junnan Li, Dongxu Li, Silvio Savarese, and Steven Hoi. Blip-2: Bootstrapping language-image pre-training with frozen image encoders and large language models. In *ICML*, 2023.
- [Li *et al.*, 2023d] Kunchang Li, Yali Wang, Yizhuo Li, Yi Wang, Yanan He, Limin Wang, and Yu Qiao. Unmasked teacher: Towards training-efficient video foundation models. In *ICCV*, 2023.
- [Li *et al.*, 2023e] Yicong Li, Junbin Xiao, Chun Feng, Xiang Wang, and Tat-Seng Chua. Discovering spatio-temporal rationales for video question answering. In *ICCV*, 2023.
- [Liu *et al.*, 2023] Haotian Liu, Chunyuan Li, Qingyang Wu, and Yong Jae Lee. Visual instruction tuning. In *NeurIPS*, 2023.
- [Park *et al.*, 2021] Jungin Park, Jiyoung Lee, and Kwanghoon Sohn. Bridge to answer: Structure-aware graph interaction network for video question answering. In *CVPR*, 2021.
- [Peng *et al.*, 2022] Min Peng, Chongyang Wang, Yuan Gao, Yu Shi, and Xiang-Dong Zhou. Multilevel hierarchical network with multiscale sampling for video question answering. In *IJCAI*, 2022.
- [Radford *et al.*, 2021] Alec Radford, Jong Wook Kim, Chris Hallacy, Aditya Ramesh, Gabriel Goh, Sandhini Agarwal, Girish Sastry, Amanda Askell, Pamela Mishkin, Jack Clark, et al. Learning transferable visual models from natural language supervision. In *ICML*, 2021.
- [Touvron *et al.*, 2023] Hugo Touvron, Thibaut Lavril, Gautier Izacard, Xavier Martinet, Marie-Anne Lachaux, Timothée Lacroix, Baptiste Rozière, Naman Goyal, Eric Hambro, Faisal Azhar, et al. Llama: Open and efficient foundation language models. *arXiv preprint arXiv:2302.13971*, 2023.
- [Vaswani *et al.*, 2017] Ashish Vaswani, Noam Shazeer, Niki Parmar, Jakob Uszkoreit, Llion Jones, Aidan N Gomez, Łukasz Kaiser, and Illia Polosukhin. Attention is all you need. In *NeurIPS*, 2017.
- [Wang *et al.*, 2022] Yi Wang, Kunchang Li, Yizhuo Li, Yanan He, Bingkun Huang, Zhiyu Zhao, Hongjie Zhang, Jilan Xu, Yi Liu, Zun Wang, et al. Internvideo: General video foundation models via generative and discriminative learning. *arXiv preprint arXiv:2212.03191*, 2022.
- [Xiao *et al.*, 2021] Junbin Xiao, Xindi Shang, Angela Yao, and Tat-Seng Chua. Next-qa: Next phase of question-answering to explaining temporal actions. In *CVPR*, 2021.
- [Xiao *et al.*, 2022a] Junbin Xiao, Angela Yao, Zhiyuan Liu, Yicong Li, Wei Ji, and Tat-Seng Chua. Video as conditional graph hierarchy for multi-granular question answering. In *CVPR*, 2022.
- [Xiao *et al.*, 2022b] Junbin Xiao, Pan Zhou, Tat-Seng Chua, and Shuicheng Yan. Video graph transformer for video question answering. In *ECCV*, 2022.
- [Xiao *et al.*, 2023] Junbin Xiao, Angela Yao, Yicong Li, and Tat Seng Chua. Can i trust your answer? visually grounded video question answering. *arXiv preprint arXiv:2309.01327*, 2023.
- [Xu *et al.*, 2017] Dejing Xu, Zhou Zhao, Jun Xiao, Fei Wu, Hanwang Zhang, Xiangnan He, and Yueting Zhuang. Video question answering via gradually refined attention over appearance and motion. In *ACM MM*, 2017.
- [Xu *et al.*, 2023a] Haiyang Xu, Qinghao Ye, Ming Yan, Yaya Shi, Jiabo Ye, Yuanhong Xu, Chenliang Li, Bin Bi, Qi Qian, Wei Wang, et al. mplug-2: A modularized multimodal foundation model across text, image and video. *arXiv preprint arXiv:2302.00402*, 2023.
- [Xu *et al.*, 2023b] Jiaqi Xu, Bo Liu, Yunkuo Chen, Mengli Cheng, and Xing Shi. Multi: Efficient video-and-language understanding with multiway-sampler and multiple choice modeling. *arXiv preprint arXiv:2303.05707*, 2023.
- [Yang *et al.*, 2021] Antoine Yang, Antoine Miech, Josef Sivic, Ivan Laptev, and Cordelia Schmid. Just ask: Learning to answer questions from millions of narrated videos. In *CVPR*, 2021.
- [Yang *et al.*, 2022] Antoine Yang, Antoine Miech, Josef Sivic, Ivan Laptev, and Cordelia Schmid. Zero-shot video question answering via frozen bidirectional language models. In *NeurIPS*, 2022.
- [Ye *et al.*, 2022] Qinghao Ye, Guohai Xu, Ming Yan, Haiyang Xu, Qi Qian, Ji Zhang, and Fei Huang. Hitea: Hierarchical temporal-aware video-language pre-training. *arXiv preprint arXiv:2212.14546*, 2022.
- [Ye *et al.*, 2023] Qinghao Ye, Haiyang Xu, Guohai Xu, Jiabo Ye, Ming Yan, Yiyang Zhou, Junyang Wang, Anwen Hu, Pengcheng Shi, Yaya Shi, et al. mplug-owl: Modularization empowers large language models with multimodality. *arXiv preprint arXiv:2304.14178*, 2023.
- [Yu *et al.*, 2019] Zhou Yu, Dejing Xu, Jun Yu, Ting Yu, Zhou Zhao, Yueting Zhuang, and Dacheng Tao. Activitynet-qa: A dataset for understanding complex web videos via question answering. In *AAAI*, 2019.
- [Yu *et al.*, 2023] Shoubin Yu, Jaemin Cho, Prateek Yadav, and Mohit Bansal. Self-chained image-language model for video localization and question answering. In *NeurIPS*, 2023.
- [Zang *et al.*, 2023] Chuanqi Zang, Hanqing Wang, Mingtao Pei, and Wei Liang. Discovering the real association: Multimodal causal reasoning in video question answering. In *CVPR*, 2023.
- [Zhang *et al.*, 2023] Hao Zhang, Aixin Sun, Wei Jing, and Joey Tianyi Zhou. Temporal sentence grounding in videos: A survey and future directions. *IEEE TPAMI*, 2023.
- [Zheng *et al.*, 2023] Lianmin Zheng, Wei-Lin Chiang, Ying Sheng, Siyuan Zhuang, Zhanghao Wu, Yonghao Zhuang, Zi Lin, Zhuohan Li, Dacheng Li, Eric P Xing, Hao Zhang, Joseph E. Gonzalez, and Ion Stoica. Judging llm-as-a-judge with mt-bench and chatbot arena. *arXiv preprint arXiv:2306.05685*, 2023.